

Hierarchical learning of grids of microtopics

Nebojsa Jojic

Microsoft Research, Redmond, USA

JOJIC@MICROSOFT.COM

Alessandro Perina

Istituto Italiano di Tecnologia, Genoa, Italy

ALESSANDRO.PERINA@IIT.IT

Dongwoo Kim

KAIST, Daejeon, Korea

DONGWOO.KIM@GMAIL.COM

Abstract

The counting grid is a grid of sparse word/feature distributions, called *microtopics*. A generative model does not use these microtopics individually, rather it groups them in overlapping rectangular windows and uses these grouped microtopics as either mixture or admixture components. This paper builds upon the basic counting grid model and it shows that hierarchical reasoning helps avoid local minima, produces better classification accuracy and, most interestingly, allows for extraction of large numbers of coherent microtopics from small datasets. We evaluate this in terms of consistency, diversity and clarity of the indexed content, as well as in a user study on word intrusion tasks. Finally, we also discuss interesting parallels between these models and other deep architectures.

1. Introduction

Recently, a new breed of topic models, dubbed counting grids (Jojic & Perina, 2011; Perina et al., 2013), has been introduced. These models are based on a grid of word distributions, which can best be thought of as the grounds for a massive Venn diagram of documents. Fig. 8, shows an example; the intersections among multiple documents, represented as a bag of words, create little intersection units with very small number of words in them (or rather, very sparse distribution of the words). The grid arrangement of these sparse distributions, which we will refer to here as *microtopics*, facilitates fast cumulative sum based inference and learning algorithms that chop up the documents

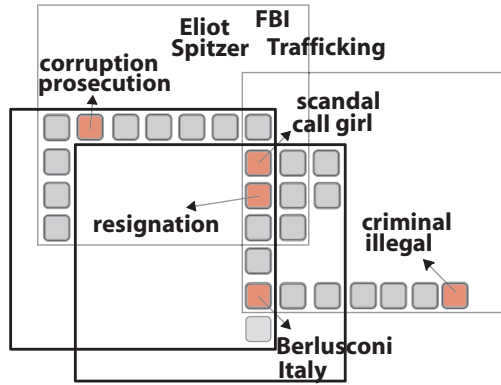


Figure 1. Counting grid as a model of sparse intersections: A Venn diagram in which documents (word sets) intersect over discrete intersection units, each containing a small number of words

into much smaller constitutive pieces than what traditional topic models typically do. For example, Fig. 3 shows part of the grid with a few representative words with greatest probability from each, and the color labeling of the grid based on the correspondence to topics from the LDA model that best fit corpus of Science magazine papers on which the grid was trained. It is immediately evident that these 2D representations can have great use in data visualization, though the model can be trained for arbitrary dimensionality (Jojic & Perina, 2011).

In these models, an individual microtopic at location $\mathbf{i} = (i_r, i_c)$, is a discrete distribution $\pi_{\mathbf{i}}(z)$ over features indexed by z , but microtopics are used in overlapping groups as defined by a rectangular window into the grid, again facilitating fast cumulative sum operations in learning and inference. The grid itself is toroidal so in a grid of size $\mathbf{E} = 32 \times 32$ there are 1024 microtopics, but also 1024 windows of any given size, (e.g. $\mathbf{W} = 8 \times 8$) that by aggregating $\pi_{\mathbf{i}}$ s, define much less sparse distributions $h_{\mathbf{i}}(z) = \frac{1}{|\mathbf{W}|} \sum_{\mathbf{j} \in W_{\mathbf{k}}} \pi_{\mathbf{j}}(z)$, where $W_{\mathbf{k}}$ is the window placed at po-

Hierarchical learning of grids of microtopics

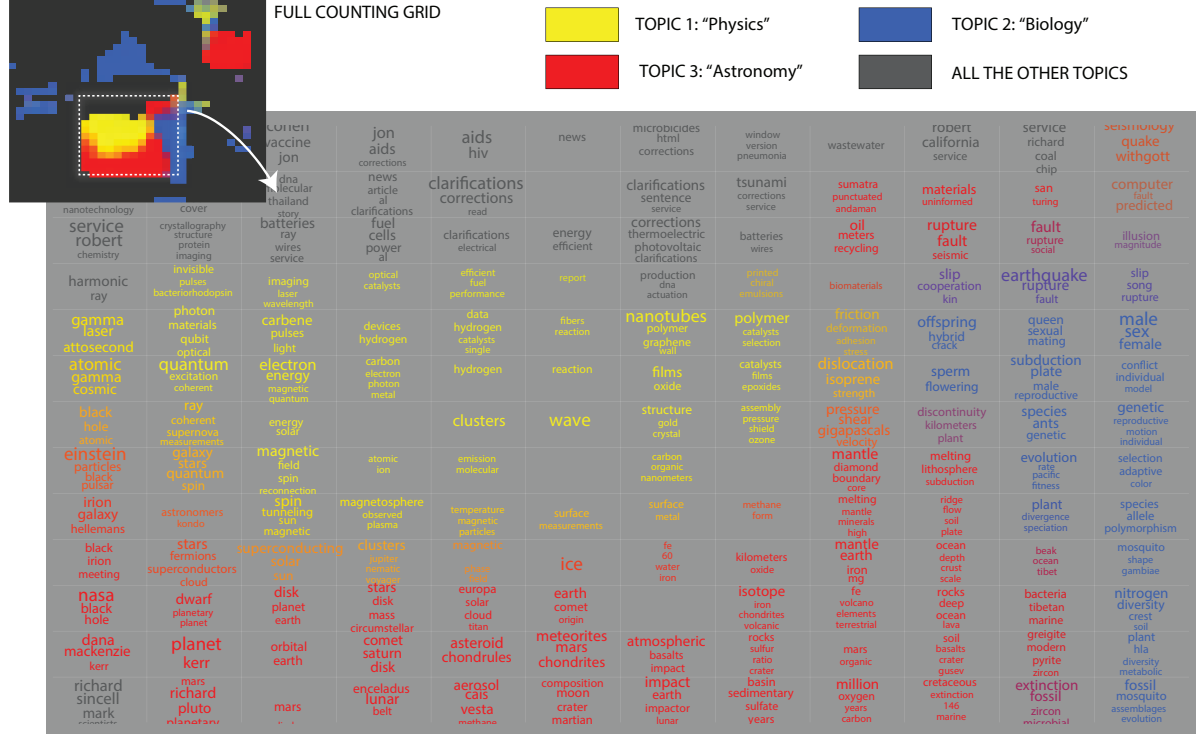


Figure 3. Clash of topics: LDA topics are mapped onto a counting grid. As visible in the top left panel, LDA's topics cluster in contiguous areas on the grid. In the zoomed in part of the grid, for each microtopic we show the most likely words if they exceed a threshold.

sition k. Fig. 2 illustrated the h -distributions¹: We show a portion of a 48×48 grid of strokes π learned from 2000 MNIST digits using a CG model assuming a 6×6 window averaging. As the CG model works with bags of features, we represented each digit as a set of pixel locations hit by a virtual photon. If a location has intensity 0.8, then it was assumed to have been hit by 8 photons and this location will appear in the bag 8 times. In other words, the histogram of features is simply proportional to the unwrapped image, and the individual distributions π or h (Eq. 1) can be shown as images by reshaping the learned histograms, as shown in each square of Fig. 2c. Finally the c-panel of Fig. 2, shows h , the aggregate distributions in the green and the red windows, as visible the depict respectively a “3” and “2”. In the same figure, the blue area show the sum of all strokes in the intersection of the two windows. The composite image with corresponding color coding is also shown in Fig. 2d; blue and red make a two, and blue and green make a three.

Due to the componential nature of the model, h contains rather sparse features (and the features in π are even sparser - only 3-4 pixels each). However, nearby features h are highly related to each other as they are the result of adding up features in overlapping windows over π .

¹High-Def. version of Fig. 2 in the appendix

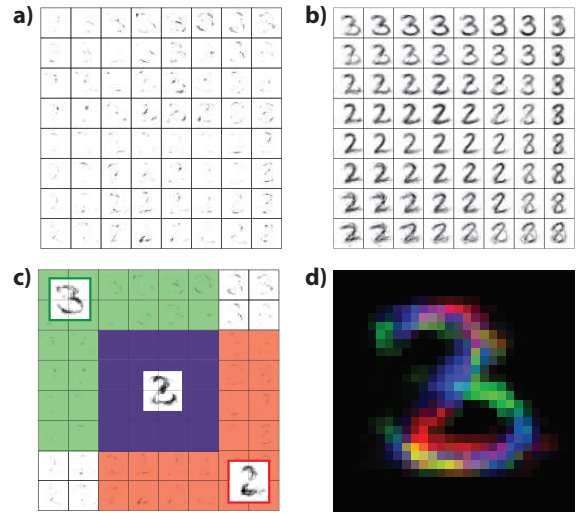


Figure 2. Intersecting digits on a grid of strokes. In this case, the data is represented by counts (intensity) associated with each image location. a) π -distribution b) h -distribution c-d) Intersecting digits

Therefore, two main differences set this type of models from other topic models: *i*) They consist of a very large number of sparse topics (microtopics) and *ii*) Nevertheless, they can be trained on much smaller datasets than would be

possible with traditional topic models with the same number of topics. This is because the use of the microtopics is highly constrained as they are used in large contiguous groups from an n -dimensional grid.

The basic counting grid (CG) model (Jojic & Perina, 2011) assumes that each document is generated from one of these h distributions, while the componential counting grid (CCG) model (Perina et al., 2013) is an admixture where each document uses words from multiple windows but not too many, as constrained by the Dirichlet prior in the same mathematical way LDA constrains the topic usage.

Therefore, if the model uses 8×8 windows, than π distributions are 64 times sparser than the h distributions, and in the basic CG model, these latter distributions should have comparable entropy to that of an individual data point indexed by t , and represented its words $\{w_n^t\}$. However, in a componential counting grid model, h distributions can be considerably sparser than the feature histograms for an individual data point. The microtopic entropy may however be inflated when a very large dataset is embedded in a small grid.

An intriguing property of these models is that even on a grid with 1024 microtopics π and just as many grouped topics h , there is no room for too many independent groups, because with a window size 8×8 , we can place only 16 windows without overlap. The ratio between grid and window size is referred to as the *capacity* of the model, and the training set size necessary to avoid overtraining the model only needs to be 1-2 orders of magnitude above the capacity number. Thus a grid of 1024 microtopics may very well be trainable with thousands of data points, rather than 100s of thousands that traditional topic models usually require!

Previous work demonstrated advantages counting grid models have in classification (Jojic & Perina, 2011), and anecdotally, in visualization/browsing tasks (Perina et al., 2014). Two interesting questions remain unanswered:

1. Are the individual microtopics meaningful even when trained on datasets that are too small for traditional models with large number of topics? Or do microtopics only make sense in overlapping groups, given that their use is thus constrained? Anecdotal evidence, e.g. Fig. 3, indicates that the finely defined microtopics and their arrangement make sense, but no direct testing of the microtopic coherence has been performed to date.
2. It is easy to imagine (and see in practice) the type of local minima counting grid models are prone to. In Fig. 3 we can imagine reshuffling of 3-4 contiguous chunks of the grid to create another grid with similar local qualities, and thus the EM learning procedure may produce results with suboptimal local likelihood

maxima. Individual microtopics may have similar levels of coherence across these local minima. But, is it also possible that better learning algorithms can produce just better arranged and more coherent microtopics than the basic EM algorithm?

This paper answers to the questions above and brings several important contributions. We introduce a family of hierarchical models of dubbed *hierarchical counting grids* - HCG and *hierarchical componential counting grids* - HCCG. Then we show how hierarchical models can be collapsed mathematically to CGs or CCGs and used to dramatically improve local maxima; in this sense HCGs and HCCGs will be also considered *hierarchical learning algorithms* to learn CGs or CCGs². This is very important, especially when variational inference is employed to learn hierarchical models (Hoffman & Blei, 2014). For example, the hierarchical counting grid model consistently outperforms traditionally trained CG model of same complexity by more than 2 standard deviations in log likelihood. As second important contribution we introduce a new test-bed to numerically evaluate the quality of a “topic” and we show that *i*) microtopics are indeed coherent and meaningful and *ii*) hierarchical models outperformed shallow grids and topic models in terms of microtopic on such measures and in 24000 subjective evaluations in a user study performed by 345 participants on Mechanical Turk.

2. Hierarchical learning of grids of microtopics

The (C)CG grids (Jojic & Perina, 2011; Perina et al., 2013): The basic counting grid π_k (Jojic & Perina, 2011) is a set of distributions on the N -dimensional discrete grid indexed by k where each $k_d \in [1 \dots E_d]$ and E describes the extent of the counting grid in d dimensions. The index z indexes a particular word in the vocabulary $z = [1 \dots Z]$. For example, $\pi_i(z)$ is the probability of the word z at the location i . Since π is a grid of distributions, $\sum_z \pi_k(z) = 1$ everywhere on the grid. The grids generate bags of words, each represented by a list of words $\{w_n\}_{n=1}^N$ and each word w_n takes a value between 1 and Z . In the rest of the paper, we will assume that all the samples have N words.

Counting Grids assume that each bag follows a word distribution found somewhere in the counting grid; in particular, using windows of dimensions W , a bag can be generated by first picking a window of size W at location ℓ , denoted as W_ℓ , then generating each of the N words by sampling k_n uniformly within the window, and finally by sampling from the distribution π_k .

Because the marginal distribution $P(k_n|\ell)$ is a preset uniform distribution over the grid locations inside the window placed at location ℓ , the model can be collapsed by summing out k_n (Jojic & Perina, 2011), and simply generating

²Indeed throughout the paper we will use hierarchical-“model”, -“learning” and -“reasoning” as synonyms

Hierarchical learning of grids of microtopics

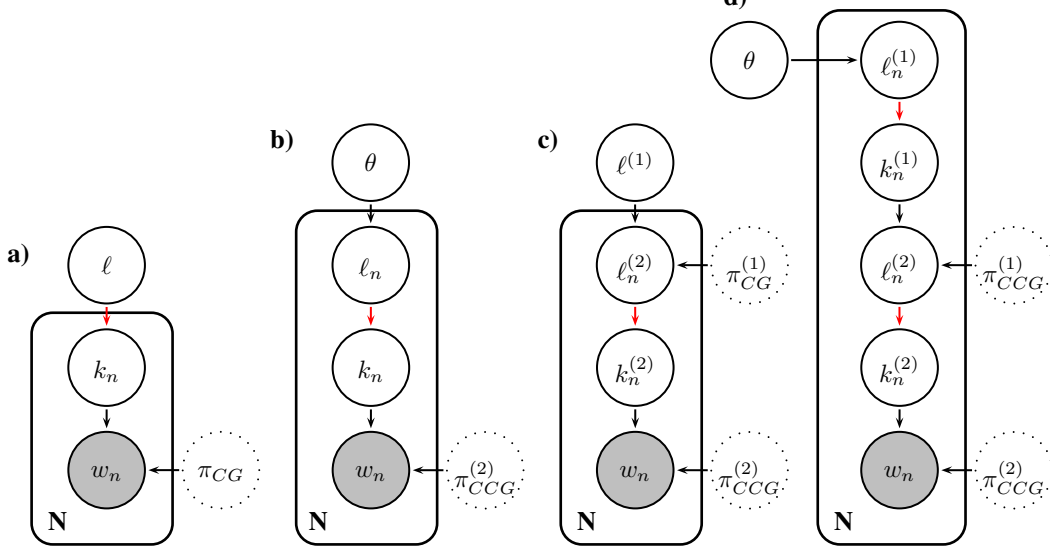


Figure 4. **a)** The basic counting grid, **b)** the componential counting grid, **c)** the hierarchical counting grid model (HCG) obtained by stacking a componential counting grid and a counting grid, and **d)** the hierarchical componential counting grid model (HCCG). Dotted circles represent the parameters of the models. Red links represent known conditional distributions $P(k_n|\ell_n) = U_\ell^W$ - Eq. 5. They are distributions over the grid locations, uniformly equal to $1/|\mathbf{W}|$ in the window of size \mathbf{W}_ℓ unequivocally identified by ℓ .

from the grouped histograms

$$h_\ell(z) = \frac{1}{|\mathbf{W}|} \sum_{j \in W_\ell} \pi_j(z) \quad (1)$$

being $|\mathbf{W}|$ is the area of the window or $\prod_d W_d$. In other words, the position of the window ℓ in the grid is a latent variable given which we can write the probability of the bag as

$$p(\{\mathbf{w}\}|\ell) = \prod_n h_\ell(z) = \prod_n \left(\frac{1}{|\mathbf{W}|} \cdot \sum_{j \in W_\ell} \pi_j(w_n) \right) \quad (2)$$

The counting grid model essentially assumes the existence of a single source (e.g., one window) for all the features in one bag, but has a very large number of (highly related) choices h to choose from. Topic models (Blei et al., 2003; Blei & Lafferty, 2005) on the other hand are admixtures that capture word co-occurrences by using a much smaller number of topics that can be more freely combined to explain a single document.

Componential Counting Grids (Perina et al., 2013) bridges both worlds, allowing multiple groups of microtopics h to be mixed to explain a single document. Thus, though an admixture, the CCG model still has a very large number of highly related topics. More precisely, each word w_n can be generated from a different window, placed at location ℓ_n , but the choice of the window follows the same prior distributions θ_ℓ for all words. Within the window at location ℓ_n the word comes from a particular grid location k_n , and from that grid distribution the word is assumed to have been generated. The probability of a bag turns to be

$$P(\{\mathbf{w}\}|\pi) = \prod_n \sum_\ell \left(\theta_\ell \cdot \left(\frac{1}{|\mathbf{W}|} \sum_{j \in W_\ell} \pi_j(w_n) \right) \right) \quad (3)$$

Both models can be learned efficiently using the EM algorithm because the inference of the hidden variables, as well as updates of π and h can be performed using summed area tables (Crow, 1984), and are thus considerably faster than most of the sophisticated sampling procedures used to train other topic models.

Hierarchical grids: By learning a model in which microtopics join forces with their neighbors to explain the data, (C-)CG models tend to exhibit high degrees of relatedness of nearby topics. As we slowly move away from one microtopic, the meaning of the topics we go over gradually shifts to related narrowly defined topics as illustrated by Fig. 3; this makes these grids attractive to HCI applications. But this also means that simple learning algorithms can be prone to local minima, as random initializations of the EM learning sometimes result in grouping certain related topics into large chunks, and sometimes breaking these same chunks into multiple ones with more potential for suboptimal microtopics along boundaries. For example, in Fig. 5a we show a 48×48 grid of strokes h (Eq. 1) learned from 2000 MNIST digits using a CCG model assuming a 5×5 window averaging³.

Due to the componential nature of the model, h contains rather sparse features (and the features in π are even sparser - only 3-4 pixels each). However, nearby features h are highly related to each other as they are the result of adding up features in overlapping windows over π . CCG is an

³we used pixels intensities as features like we explained in the introduction

admixture model, and so each digit indexed by t has a relatively rich posterior θ^t over the features in h . In Fig. 5b⁴, we show one of the main principal components of variation in θ . For three peaks there, we also show h -features at those locations and the combination of these three sparse features creates a longer contiguous stroke. Thus, the separation of these features across three distant parts of the map is likely a result of a local minimum in basic EM training.

This illustration points to an idea on how to build better models. The locations ℓ that a data point t maps to could be considered a new representation of the data point (digit in this case), with the posterior probability for each location considered a derived feature count. Thus another layer of a generative model can be added on top to generate the locations in the grid below, Fig. 4c-d. It is particularly useful to use another microtopic grid model as this added layer, rather than a linear mixing model that the PCA example above might suggest, because of the inherent relatedness of the nearby locations in the grid. In the example above, the features around the three peaks we highlight are also often correlated with each other, as a slight shift in the grid only slightly changes each of these features, leaving them equally combinable. The layer above can thus be either another admixture grid model (CCG), or a mixture (CG). As CG is a mixture model, it terminates the layering as the posterior distributions become peaky and thus uncorrelated, but an arbitrary number of CCGs can be stacked on top of each other in this manner, terminating (or not) with a CG layer.

For the sake of brevity, we only derive HCG learning algorithm. This easily generalizes to HCCG and to higher order hierarchies⁵. Variational inference and learning procedure for counting grid-based models utilizes cumulative sums and is slower than training an individual (C-)CG layer by a factor proportional to the number of layers.

The Bayesian network of HCG is shown in Fig. 4c. To simply the notation, we renamed the CG's location variable from $\ell^{(1)}$ to m ; this allows us to omit the superscript “⁽¹⁾” or “⁽²⁾” that indexes the layer.

As one would expect the conditional distributions defined by the notwork factorization, are inherited from (C-)CGs. In fact

$$P(w_n|k_n, \pi_{CCG}) = \pi_{CCG, k_n}(w_n) \quad (4)$$

is a multinomial over the vocabulary. Then

$$P(k_n|\ell_n) = U_{\ell_n}^W(k_n) = \begin{cases} \frac{1}{|\mathbf{W}|} & \text{if } k_n \in \mathbf{W}_{\ell_n} \\ 0 & \text{Otherwise} \end{cases} \quad (5)$$

is a pre-set distribution over the grid locations, uniform inside W_{ℓ_n} . Finally, the upper layer is inherited from the

⁴A bigger, higher resolution version of Fig.5 is in the appendix

⁵A general algorithm for learning higher order hierarchical grids is reported in the appendix

CGs; The location variable m does not depends on the word index n , thus

$$P(\ell_n|m, \pi_{CG}) = \frac{1}{|\mathbf{W}|} \cdot \sum_{\mathbf{k} \in W_m} \pi_{CG, \mathbf{k}}(\ell_n) \quad (6)$$

From last formula it is evident how lower-levels' locations act as observations in the higher level.

The true posterior $p(\{k_n\}, \{\ell_n\}, m|w_n, \pi_{CCG}, \pi_{CG})$ is intractable for exact inference and we resort to variational EM algorithm (Neal & Hinton, 1999). Following the variational recipe, we firstly introduce a fully factorized posterior q , approximating the true posterior as

$$q^t(\{k_n\}, \{\ell_n\}, m) = q^t(m) \cdot \prod_n (q^t(k_n) \cdot q^t(\ell_n)) \quad (7)$$

being the q 's multinomials over the grid's locations⁶. Then, we write the negative free energy \mathcal{F} which bounds the non-constant part of the loglikelihood of the data as

$$\begin{aligned} \mathcal{F} = & \sum_{t, n, k_n} q^t(k_n) \log \pi_{CCG, \mathbf{k}}(w_n^t) + \sum_{t, n, k_n, \ell_n} q^t(k_n) q^t(\ell_n) \log U_{\ell_n}^W(k_n) \\ & + \sum_{t, m, \ell_n} q^t(m) q^t(\ell_n) \log \pi_{CG, m}(\ell_n) - \mathbb{H}(q(m, \{k_n\}, \{\ell_n\})) \end{aligned}$$

where $\mathbb{H}(q(m, \{k_n\}, \{\ell_n\}))$ is the entropy of the variational posterior - Eq. 7.

Finally we maximize \mathcal{F} by means of the EM algorithm which iterates E- and M-steps until convergence. The E-step maximizes \mathcal{F} wrt to the posterior distributions given the current status of the model, and in our case reduces to the following updates:

$$\begin{aligned} q^t(k_n = \mathbf{i}) & \propto (e^{\sum_{\ell_n} q^t(\ell_n) \log U_{\ell_n}^W(\mathbf{i})}) \cdot \pi_{CCG, \mathbf{i}}(w_n) \\ q^t(\ell_n = \mathbf{i}) & \propto (e^{\sum_{k_n} q^t(k_n) \log U_{\mathbf{i}}^W(k_n)}) \cdot (e^{\sum_m q^t(m) \log \pi_{CG, m}(\mathbf{i})}) \\ q^t(m = \mathbf{i}) & \propto e^{\sum_n \sum_{\ell_n} q^t(\ell_n) \cdot \log h_{CG, \mathbf{i}}(\ell_n)} \end{aligned}$$

where \mathbf{i} is an index that represents a generic position in the grid. The M step re-estimate the model parameters using these updated posteriors:

$$\begin{aligned} \pi_{CCG, \mathbf{i}}(z) & \propto \sum_t \sum_n q^t(k_n = \mathbf{i}) \cdot [w_n^t = z] \\ \pi_{CG, \mathbf{i}}(1) & \propto \hat{\pi}_{CG, \mathbf{i}}(1) \cdot \sum_{t, n} q^t(\ell_n = 1) \cdot \sum_{\mathbf{k} | \mathbf{i} \in W_{\mathbf{k}}} \hat{h}_{CG, \mathbf{i}}(1) \end{aligned}$$

where we refer the reader to (Jojic & Perina, 2011) for details on the last update. As it is performed directly from the collapsed version the CG model, it requires a second variational bound for the presence of a summation over the grid positions within windows \mathbf{W} - (see Eq. 2).

Interestingly, however, training these hierarchical models stage by stage, by feeding $L^t = \sum_n q^t(\ell_n)$ or a smoothed

⁶ Eventually each level's grid can have different size, similar in spirit to autoencoders, although we didn't consider this here

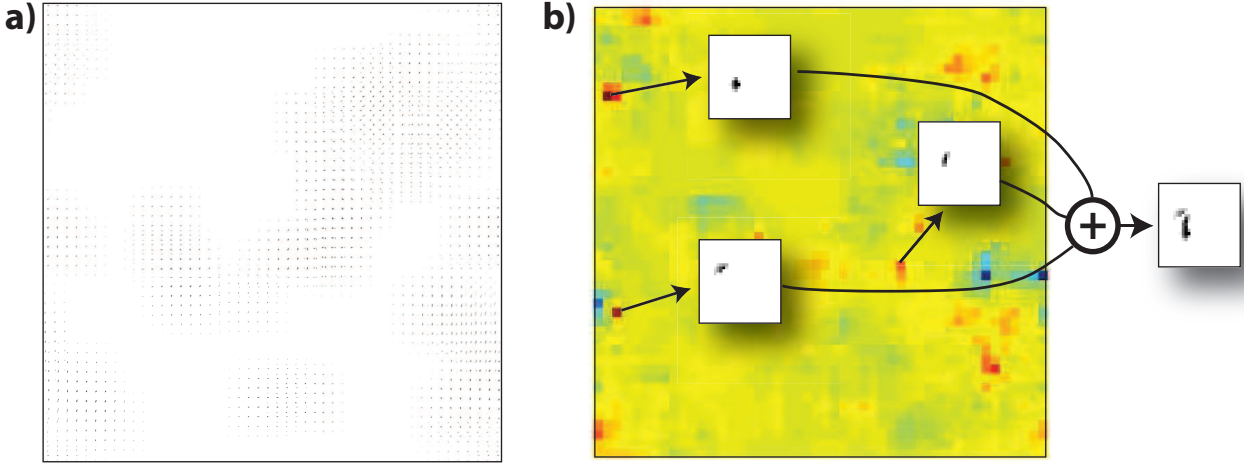


Figure 5. The benefits of hierarchical learning: **a)** h_{CCG} - a bigger higher resolution version in the appendix. **b)** Principal components of θ and three peaks put together.

version of it from one stage as input to the next works well. This is reminiscent of deep models where such incremental learning was practically useful (Hinton & Osinero, 2006).

As opposed to the usual applications of deep models, the deep CCG models can actually be directly simplified into a single layer CCG or CG model which is then easier to visualize. Although it has been shown that a deep neural network can be compressed into a shallow broader one through post training (Ba & Caurana, 2013), the stacked (C-)CG models can be collapsed mathematically; the model on top will dictate the nature of the resulting model. In this sense we can view HCG and HCCG as *hierarchical learning algorithms*. For example, for HCG in Fig. 4c-d, it straightforward to see that the following grid defined over the original features $\{w_n\}$,

$$\pi_\ell(w_n) = \sum_i \pi_{i,\ell}^{(1)}(\mathbf{i}) \cdot h_{CCG,i}^{(2)}(w_n) \quad (8)$$

can be used as a single layer grid that describes the same data distribution as the two-layer model⁷.

However, the grids estimated from the hierarchical models should be more compact as the scattered groups of features are progressively merged in each new layer. *Learning in hierarchical models is thus more gradual and results in better local maxima, and we show below that the results are far superior to regular EM learning of the collapsed CG or CCG models.*

3. Experiments

Likelihood comparison: As first experiment we compared the local maxima on MNIST dataset. The 2-layers HCG model trained stage-wise, and refined by further EM training, starting with 20 random initializations consistently produced higher likelihood than the CG models di-

rectly learned by 20 times randomly initialized EM. In fact, no single CG learned by collapsing HCG had log likelihood less than two standard deviations above the highest log likelihood learned by basic EM ($p\text{-value} < 1e-20$). Both approaches were trained with the computation time equivalent to 1000 iterations of standard EM, which was more than enough for convergence.

Evaluation microtopic quality: We evaluated the coherence and the clarity of the microtopics comparing the collapsed (2 layers) hierarchical grids - HCG and HCCG, with regular grids (Jojic & Perina, 2011; Perina et al., 2013), latent Dirichlet allocation - LDA (Blei et al., 2003), the correlated topic model - CTM (Blei & Lafferty, 2005) which allows to learn a large set of correlated topics and few non parametric topic models (Paisley et al., 2012; Teh et al., 2004).

This section has also the benefit of proposing a novel evaluation procedure for topic models which is strongly related to information indexing. Evaluation of topic models usually is made in terms of perplexity, however different models, even different learning algorithm of the same model, are very difficult to compare (Asuncion et al., 2009) and the better perplexity does not always indicates the better human readable topics (Chang et al., 2009). This motivated us to propose an additional evaluation procedure.

In our experiment, we considered a corpus \mathcal{D} composed of Science Magazine reports and scientific articles from the last 20 years. This is a very diverse corpus similar to the one used in (Blei & Lafferty, 2005). As preprocessing step, we removed stop-words and applied the Porters' stemmer algorithm (Porter, 1997).

We considered grids of size 16×16 , 24×25 , 32×32 , 40×40 and 48×48 fixing the window size to 5×5 . Previous literature showed indeed that counting grids are only sensi-

⁷ h_i are the grouped microtopics in the window \mathbf{W}_i - Eq. 1

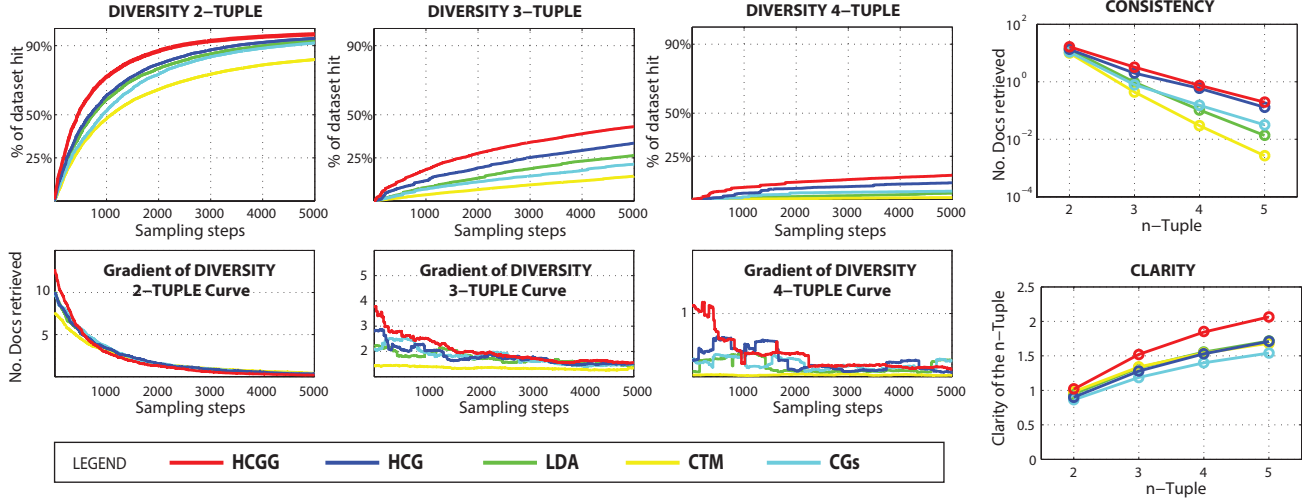


Figure 6. Microtopic evaluations. We compared 32×32 grids with the *best* result obtained by LDA and CTM. To avoid cluttering the graph, we did not report CGs results which were found inferior to the proposed hierarchical models. We also reported the gradient of the diversity curves to show that new samples steadily continue to contribute new tuples.

tive to the ratio between grid and window area, once windows are sufficiently big. We varied number of topics for LDA and CTM in $\{10, 15, \dots, 100, 125, 150, \dots, 1000\}$. We learned each model 5 times and we averaged the results. In each repetition, we considered a random third of this corpus, for total of roughly $|\mathcal{D}| = 12K$ documents, $Z = 20K$ different words and more than $600K$ tokens.

To evaluate (micro)topics, we repetitively randomly sampled k -tuples of words and checked for consistency, diversity and clarity of the indexed content. In the following, we describe the procedure used for evaluating grids; the generalization to topic models is straightforward.

To pick a tuple \mathcal{T} of n words, we sampled a grid location $\hat{\ell}$ from an uniform distribution⁸. Then, we repetitively sampled the microtopic $\pi_{\hat{\ell}}$ to obtain the words in the tuple $\mathcal{T} = \{w_1, \dots, w_n\}$. We did not allow repetitions of words in the tuple. We considered 5000 different $n = 2, 3, 4, 5$ -tuples, not allowing repeated tuples.

Then we checked for consistency, diversity and clarity of content indexed by each tuple. The **consistency** is quantified in terms of the average number of documents from the dataset that contained *all* words in \mathcal{T} . The **diversity** of indexed content is illustrated through the cumulative graph of acquired unique documents as more and more n -tuples are sampled and used to retrieve documents containing them⁹. As this last curve depends on the sample order, we further repeated the process 5 times for a total of 25K different samples. Finally the **clarity** (Cronen-Townsend & Croft, 2002), measures the ambiguity of a query with respect to a collection of documents and it has been used to identify ineffective queries, on average, without relevance information. More formally, the clarity is measured as the entropy between the n -tuple and the language model $P(w)$ (uni-

gram distributions).

$$\text{Clarity} = \sum_w P(w|T) \cdot \log_2 \frac{P(w|T)}{P(W)} \quad (9)$$

where $P(w|T) = \sum_{d \in \mathcal{D}} P(w|\mathcal{D}) \cdot P(\mathcal{D}|T)$. We estimated the likelihood of an individual document model generating the tuple $P(T|\mathcal{D}) = \prod_{w_t \in T} P(w_t|\mathcal{D})$ and obtain $P(\mathcal{D}|T)$ using uniform prior probabilities for documents that contains a word in the tuple, and a zero prior for the rest. Finally, to estimate $P(w|T)$ we employed MonteCarlo sampling using 500 samples.

Results are illustrated in Fig.6 and must appreciated by looking at all three measures together. We report results for the 32×32 grids and the best result of LDA and CTM which both peaked at around 80 topics. Results for other sizes can be found in the additional material; they are stable across complexities with slightly better performances for larger grids.

All grid models show good consistency of words selected as they are optimized so that documents' words map into overlapping windows, and so through the positioning and intersection of many related documents the words should end up being arranged in a fine-grained manner so as to reflect their higher-order co-occurrence statistics. Hierarchical learning greatly improved the results despite the fact that HCCG and HCG can be reduced to (C)CGs as previously shown.

Overall HCCG strongly outperformed all the methods, especially with a total gain of 0.5 bits on clarity, which is around third of the score for LDA/CTM. Despite allowing for correlated topics that enable CTM to learn larger topic models, CTM trails LDA in these graphs as topics were overexpanded. We also considered non-parametric topic

⁸we also tried sampling from the appropriate learned prior distribution, but results were found to be lower

⁹e.g., How many samples do we need to hit the whole corpus

models such as “Dilan” (Paisley et al., 2012) and the hierarchical Dirichlet process (Teh et al., 2004) but their best results were poor and we did not report them in the figure. To get an idea, both models only indexed 25% of the content after 5000 2-Tuples samples and had a clarity lower of 0.7-1.2 bits than other topic models.

User studies: We performed a *word intrusion* task (Chang et al., 2009), originally developed to measure the coherence of topics with large scale user study, and later adopted to various measures of the topic coherence (Reisinger et al., 2010).

In the original word intrusion task, six randomly ordered words are presented to a subject and the task of the user is to find the word which is an outlier. In the original procedure a target topic is randomly selected and then the five words with highest probability are picked. Then, an intruder is added to this set, selecting a word at random from the low probability words of the target topic, but high probability in some other topic. Finally the six words are shuffled and presented to the subject. If the target topic shows a lack of coherence, the subject will often fail to correctly detect the intruder.

Apart from microtopic models, the best performing model in the previous section was found to be LDA with a much smaller number of topics than, for instance a HCCG. Thus the question is if the fine tessellation of gross topics that HCCG performs well (in numerical sense) actually produces topics that are meaningful to humans, or are these distinctions artificial in that sampling words from LDA topics would create no more nor less coherent subtopics than the ones laid out on our grids.

Thus instead of picking the top words from each topic, we sampled the words from the target topic to create the ingroup. After sampling the location of a microtopic from the grid $\hat{\ell}$, we picked three randomly chosen words again from $\pi_{\hat{\ell}}$ and from the “averaged” microtopic started from the selected location to window of size 2×2 , and 3×3 , respectively. We choose the intruder word using the standard procedure. We compared LDA (known to performed better than CTM on such task (Chang et al., 2009)), HCG, and HCCG, on randomly crawled 10K Wikipedia articles and used Amazon Mechanical Turk (<http://www.mturk.com>) receiving 24000 hits from 345 different people.

Results are shown in Fig.11 as a function of the euclidean distance on the grid. HCCG outperformed with LDA (p-values for the 3 tasks 1.20e-11, 1.88e-5, 2.97e-05) and HCG (p-values for the 3 tasks 3.97e-18, 1.01e-11, 3.14e-19). Overall, users were able to solve correctly 71% of HCCG problems and only 58% of LDA problems. More interestingly the performance of HCCG and HCG does not depend on the distance and even picking intruder word from a close location didn’t confuse the users! This shows that HCCG chops up the data into meaningful microtopics

	CG	HCG	CCG	HCCG	LDA
20N	92,31%	93,49%	93,41%	95,01%	89,23%
MC	38,73%	38,91%	76,22%	78,94%	72,21%

Table 1. Document classification. When bold, hierarchical grids outperformed the basic grids with statistical significance (HCG p-value = 2.01e-4, HCCG p-values < 1e-3).

which are then combined into a large number of groups h that do not overbroaden the scope as CTM did in our experiments. Finally, it is worth to note that HCCG and HCG outperformed respectively CG and CCG and the results are reported in the appendix.

Document classification: Although we were primarily considering how these various models capture the correlations in the data, as final test we also evaluated the benefits of hierarchical reasoning in classification. We considered the 20-newsgroup dataset¹⁰ (20N) and the Mastercook dataset¹¹ (MC) composed by 4000 recipes divided in 15 classes. Previous work (Banerjee & Basu, 2007; Reisinger et al., 2010) reduced 20-Newsgroup dataset into subsets with varying similarities and we considered the hardest subset composed by posts from the very similar newsgroups `comp.os.ms-windows`, `comp.windows.x` and `comp.graphics`. We considered the same complexities as in the numerical evaluation of microtopics above, using 10-fold crossvalidation and classified test document using maximum likelihood. Results for both datasets are shown in Tab. 1.

4. Conclusions

We show that with new learning algorithms based on a hierarchy of CCG model, possibly terminated on the top with a CG, it is possible to learn large grids of sparse related microtopics from relatively small datasets. These microtopics correspond to intersections of multiple documents, and are considerably narrower than what traditional topic models can achieve without overtraining on the same data. Yet, these microtopics are well formed, as both the numerical measures of consistency, diversity and clarity and the user study on 345 mechanical turkers show. Another approach to capturing sparse intersections of broader topics is through product of expert models, e.g. RBMs (Salakhutdinov & Hinton, 2009), which consist of relatively broad topics but model the data through intersections rather than admixing. RBMs are also often stacked into deep structures. In future work it would be interesting to compare these models, though the tasks we used here

¹⁰<http://www.cs.cmu.edu/afs/cs.cmu.edu/project/theo-20/www/data/news20.html>

¹¹(Perina et al., 2013) - <http://www.alessandroperina.com>

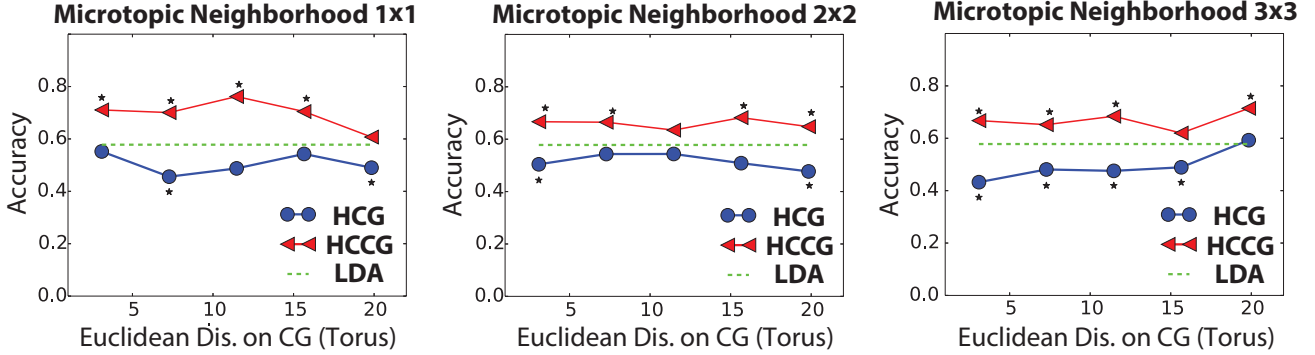


Figure 7. Result of word intrusion task. Statistical significance is denoted by *. *p*-values and further details on the test are reported in the appendix

would have to be somewhat changed to focus on the intersection modeling, rather than the topic coherence (as this is not what RBM topics are optimized for). HCCG and HCG models, have a clear advantage in that it is easy to visualize how the data is represented, which is useful both to end users in HCI applications, as well as to machine learning experts for model development and debugging. Another parallel between the stacks of CCGs and other deep models is that the uniform connectivity of units is directly enforced through window constraints, rather than encouraged by dropout.

References

Asuncion, Arthur, Welling, Max, Smyth, Padhraic, and Teh, Yee Whye. On smoothing and inference for topic models. In *In Proceedings of Uncertainty in Artificial Intelligence*, 2009.

Ba, Lei Jimmy and Caurana, Rich. Do deep nets really need to be deep? *CoRR*, abs/1312.6184, 2013.

Banerjee, Arindam and Basu, Sugato. Topic models over text streams: a study of batch and online unsupervised learning. In *In Proc. 7th SIAM Intl. Conf. on Data Mining*, 2007.

Blei, D., Ng, A., and Jordan, M. Latent dirichlet allocation. *Journal of machine Learning Research*, 3:993–1022, 2003.

Blei, David M. and Lafferty, John D. Correlated topic models. In *NIPS*, 2005.

Chang, Jonathan, Boyd-Graber, Jordan L., Gerrish, Sean, Wang, Chong, and Blei, David M. Reading tea leaves: How humans interpret topic models. In *NIPS*, 2009.

Cronen-Townsend, Steve and Croft, W. Bruce. Quantifying query ambiguity. In *Proceedings of the Second International Conference on Human Language Technology Research*, HLT '02, pp. 104–109, San Francisco, CA, USA, 2002. Morgan Kaufmann Publishers Inc.

Crow, Franklin C. Summed-area tables for texture mapping. In *Proceedings of the 11th Annual Conference on Computer Graphics and Interactive Techniques*, SIGGRAPH '84, pp. 207–212, New York, NY, USA, 1984. ACM. ISBN 0-89791-138-5. doi: 10.1145/800031.808600.

Hinton, Geoffrey and Osinero, Simon. A fast learning algorithm for deep belief nets. *Neural Computation*, 18, 2006.

Hoffman, Matt and Blei, David. Structured stochastic variational inference. *CoRR*, abs/1404.4114, 2014.

Jojic, Nebojsa and Perina, Alessandro. Multidimensional counting grids: Inferring word order from disordered bags of words. In *Proceedings of conference on Uncertainty in artificial intelligence (UAI)*, pp. 547–556, 2011.

Neal, Radford M. and Hinton, Geoffrey E. A view of the em algorithm that justifies incremental, sparse, and other variants. *Learning in graphical models*, pp. 355–368, 1999.

Paisley, John, Wang, Chong, and Blei, David M. The discrete infinite logistic normal distribution. *Bayesian Analysis*, 7(4): 997–1034, 12 2012. doi: 10.1214/12-BA734.

Perina, Alessandro, Jojic, Nebojsa, Bicego, Manuele, and Truski, Andrzej. Documents as multiple overlapping windows into grids of counts. In Burges, C.J.C., Bottou, L., Welling, M., Ghahramani, Z., and Weinberger, K.Q. (eds.), *Advances in Neural Information Processing Systems 26*, pp. 10–18. Curran Associates, Inc., 2013.

Perina, Alessandro, Kim, Dongwoo, Truski, Andrzej, and Jojic, Nebojsa. Skim-reading thousands of documents in one minute: Data indexing and visualization for multifarious search. In *Workshop on Interactive Data Exploration and Analytics (IDEA'14) at KDD*, 2014.

Porter, M. F. Readings in information retrieval. chapter An Algorithm for Suffix Stripping, pp. 313–316. Morgan Kaufmann Publishers Inc., San Francisco, CA, USA, 1997. ISBN 1-55860-454-5.

Reisinger, Joseph, Waters, Austin, Silverthorn, Brian, and Mooney, Raymond J. Spherical topic models. In *ICML '10: Proceedings of the 27th international conference on Machine learning*, 2010.

Salakhutdinov, Ruslan and Hinton, Geoffrey. Replicated softmax: an undirected topic model. In *In Advances in Neural Information Processing Systems*, NIPS, 2009.

Teh, Yee Whye, Jordan, Michael I., Beal, Matthew J., and Blei, David M. Hierarchical dirichlet processes. *Journal of the American Statistical Association*, 101, 2004.

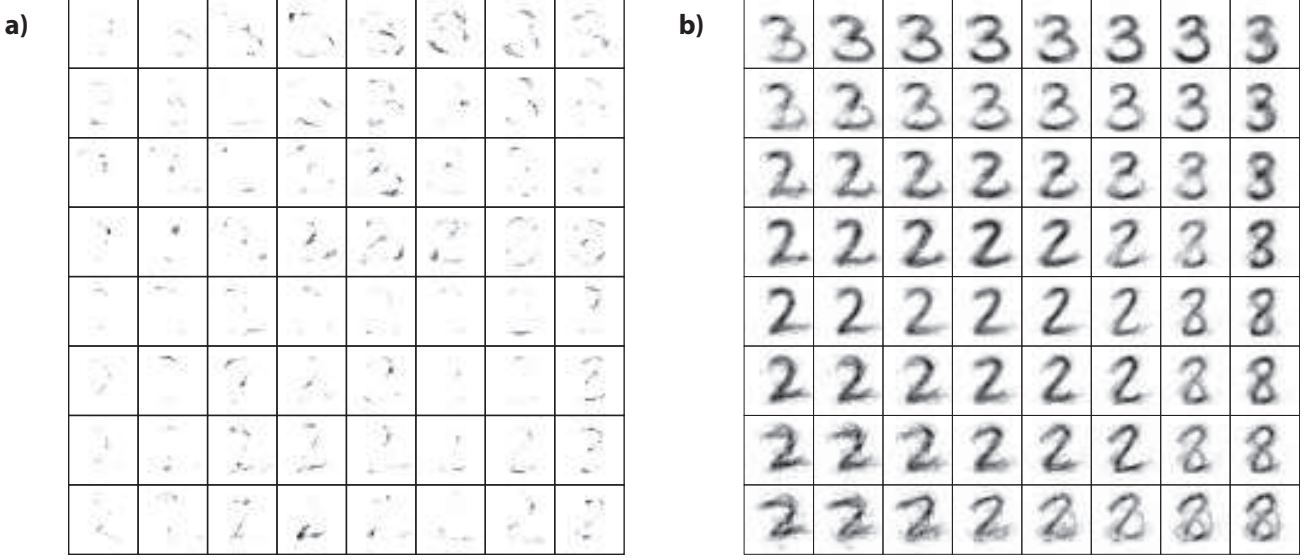


Figure 8. Grid-of-strokes. a) π , b) h . This is the Higher resolution version of Fig. 2 of the main paper

Appendix A - Grids of strokes

In this first section we report the higher resolution version of Fig. 2 and 5 in the main paper.

We considered 2000 MNIST digits: As the CG model works with bags of features, we represented each digit as a set of pixel locations hit by a virtual photon. If a location has intensity 0.8, then it was assumed to have been hit by 8 photons and this location will appear in the bag 8 times. In other words, the histogram of features is simply proportional to the unwrapped image, and the individual distributions π or h can be shown as images by reshaping the learned histograms.

In Fig. 8, We show a portion of a 48×48 grid of strokes π learned using a CG model assuming a 6×6 window averaging. Due to the componential nature of the model, h contains rather sparse features (and the features in π are even sparser - only 3-4 pixels each). However, nearby features h are highly related to each other as they are the result of adding up features in overlapping windows over π .

In Fig. 9 we show a full 48×48 grid of strokes h learned from 2000 MNIST digits using a CCG model assuming a 5×5 window averaging¹².

Due to the componential nature of the model, h contains rather sparse features (and the features in π are even sparser - only 3-4 pixels each). However, nearby features h are highly related to each other as they are the result of adding up features in overlapping windows over π . CCG is an

¹²we used pixels intensities as features like we explained in the introduction

admixture model, and so each digit indexed by t has a relatively rich posterior θ^t over the features in h .

Appendix B - Variational EM for general hierarchical grids

In the main paper we presented two hierarchical models, HCG and HCCG; the former is built stacking a CCG and a CG, the latter stacking two CCGs models. Nevertheless, deeper models are of course possible and the aim of this section is to derive a (variational) learning algorithm for a general hierarchical model.

At first we note that as any other deep architecture, hierarchical grids are a cascade of many layers where each layer uses the output from the previous layer as input. In the specific, as illustrated by Fig. 10, we stack $L - 1$ Componential Counting Grids and we put a model on the top, either a Counting Grid or a Componential Counting Grid, for a total of L layers. The model on the top will dictate the nature of the final grid. In order to make our discussion general we allow each layer to have a different complexity $\mathbf{E}^{(l)}, \mathbf{W}^{(l)}$. Finally we use \mathbf{h}^1 to specify the set of hidden variables of the model on the top. The Bayesian network of a generic model is shown in Fig. 10a, where as illustrated, one can place either a CG (Fig. 10c) or a CCG (Fig. 10c) on the top yielding respectively to a *Hierarchical Counting Grid*, HCG or a *Hierarchical Componential Counting Grid* HCCG. As one would expect, the conditional distributions induced by the newtwork factorization are inherited by the basic grids.

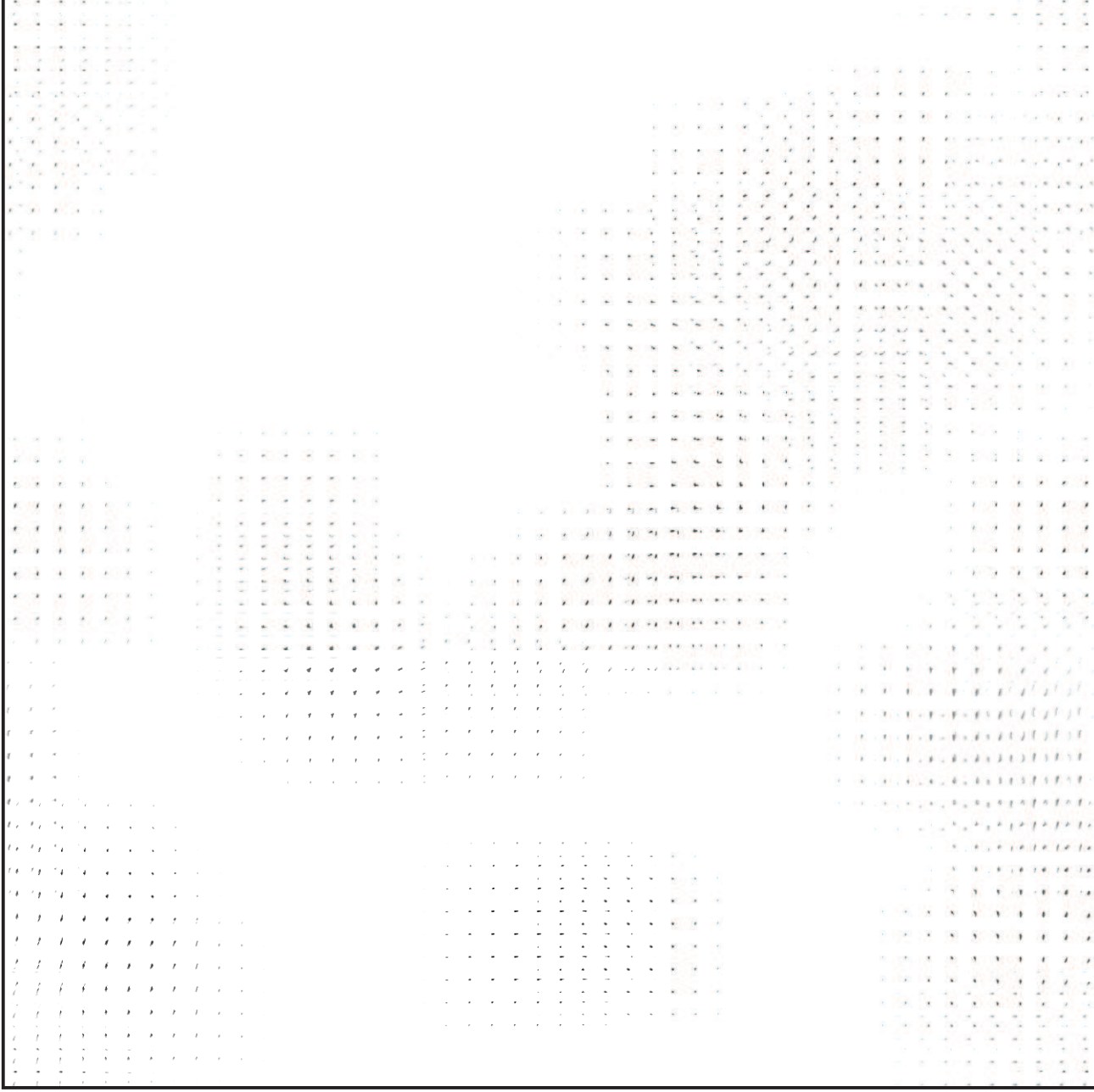


Figure 9. Grid-of-strokes. This is the Higher resolution version of Fig. 2 of the main paper

window only depends on the current grid complexity

At the bottom we have the standard obersvation model:

$$P(w_n | k_n^{(L)}, \pi^{(L)}) = \pi_{k_n}^{(L)}(w_n) \quad (10)$$

$$P(k_n^{(l)} | \ell_n^{(l)}) = U_{\ell_n^{(l)}}^{\mathbf{W}^{(l)}}(k_n^{(l)}) = \begin{cases} \frac{1}{|\mathcal{W}|} & k_n^{(l)} \in \mathbf{W}_{\ell_n^{(l)}}^{(l)} \\ 0 & \text{Otherwise} \end{cases} \quad (11)$$

where $U(\cdot)$ is a pre-set distribution, uniform with a window of size $\mathbf{W}^{(l)}$. Finally, the link between layer l and $l-1$ is

$$P(\ell_n^{(l)} | k_n^{(l-1)}, \pi^{(l-1)}) = \pi_{\ell_n^{(l-1)}}^{(l-1)}(k_n^{(l)}) \quad (12)$$

Then, within each layer l , the link between a word and its

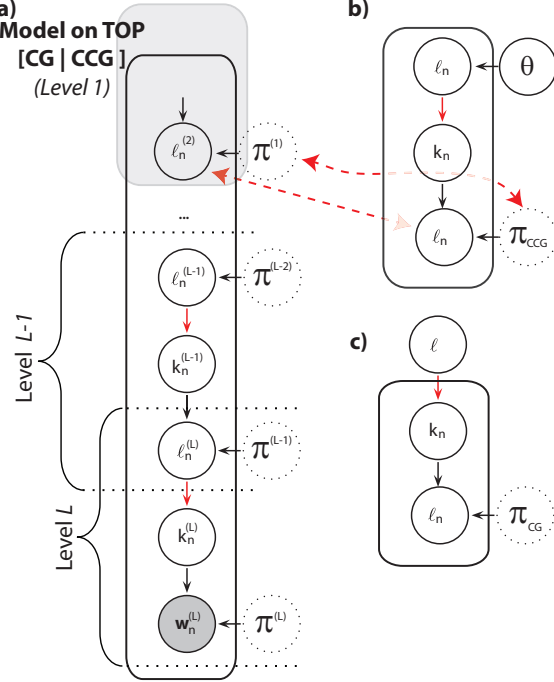


Figure 10. a) Deep hierarchical grids can be used to avoid local minima and learn better microtopics. b) The Componential Counting Grid generative model. c) The Counting Grid model

From the formula above it is evident how lower levels locations act as observations in the higher level. A Bayesian network specifies a joint distribution in the following structured form

$$P = P(\mathbf{h}^{(1)}) \cdot \prod_{n=1}^N \left(P(w_n | k_n^{(L)}, \pi^{(L)}) \cdot \prod_{l=2}^L \left(P(k_n^{(l)} | \ell_n^{(l)}) \cdot P(\ell_n^{(l)} | k_n^{(l-1)}, \pi^{(l-1)}) \right) \right) \quad (13)$$

being $P(\mathbf{h}^{(1)})$ the joint probability distribution of the hidden variables model on the top which also factorizes (Jojic & Perina, 2011; Perina et al., 2013).

The posterior $P(\{k_n^{(l)}, \ell_n^{(l)}\}, \mathbf{h}^1 | \{w_n\}, \{\pi^{(l)}\}_{l=2}^L, \pi^{(1)})$ is intractable for exact inference and we must resort to variational EM algorithm (Neal & Hinton, 1999). Following the variational recipe, we firstly introduce a fully factorized posterior q , approximating the true posterior as

$$q^t(\{k_n^{(l)}, \ell_n^{(l)}\}, \mathbf{h}^1) = q^t(\mathbf{h}^1) \cdot \prod_{l=2}^L \prod_{n=1}^N \left(q^t(k_n^{(l)}) \cdot q^t(\ell_n^{(l)}) \right)$$

and where $q^t(\mathbf{h}^1)$ is the variational posterior of the model on the top which again we assume factorized as in (Jojic & Perina, 2011; Perina et al., 2013), and where each of the q 's is a multinomial over the grids locations.

Following the standard variational recipe, we bound the

non-constant part of the loglikelihood of the data with the free energy

$$\log P(\{w_n^t\} | \{\pi^{(l)}\}_{l=1}^L) \leq \mathcal{F} = \sum_t \mathcal{F}^t \quad (14)$$

where the free energy of each t -th sample is

$$\begin{aligned} \mathcal{F}^{\perp} = & \mathbb{H}(q^t(\{k_n^{(l)}, \ell_n^{(l)}\}, \mathbf{h}^1)) - \sum_{n=1}^N \sum_{k_n=1}^{\mathbf{E}^{(L)}} q^t(k_n^{(L)}) \log \pi_{k_n}^{(L)}(w_n^t) \\ & - \sum_{l=2}^L \sum_{n=1}^N \sum_{\ell_n=1}^{\mathbf{E}^{(l)}} \sum_{k_n=1}^{\mathbf{E}^{(l)}} q^t(k_n^{(l)}) \cdot q^t(\ell_n^{(l)}) \log U_{\ell_n^{(l)}}^{\mathbf{W}^{(l)}}(k_n^{(l)}) \\ & - \sum_{l=2}^L \sum_{n=1}^N \sum_{\ell_n=1}^{\mathbf{E}^{(l-1)}} \sum_{k_n=1}^{\mathbf{E}^{(l)}} q^t(k_n^{(l)}) \cdot q^t(\ell_n^{(l-1)}) \log \pi_{\ell_n^{(l-1)}}^{(l-1)}(k_n^{(l)}) \\ & - \mathcal{F}_{q^t(\mathbf{h}^1)} \end{aligned} \quad (15)$$

In the equation above $\mathbb{H}(q^t(\{k_n^{(l)}, \ell_n^{(l)}\}, \mathbf{h}^1))$ is the entropy of the variational posterior and the last term $\mathcal{F}_{q^t(\mathbf{h}^1)}$ depends on the top model: if the model on top is a CG, we have

$$\mathcal{F}_{q^t(\mathbf{h}^1)}^{CG} = \sum_{\ell=1}^N \sum_{n=1}^{\mathbf{E}^{(1)}} \sum_{k_n=1}^{\mathbf{E}^{(1)}} q^t(k_n^{(1)}) \cdot q^t(\ell^{(1)}) \log U_{\ell^{(1)}}^{\mathbf{W}^{(1)}}(k_n^{(1)})$$

On the other hand, if the top model yet another CCG, we have

$$\begin{aligned} \mathcal{F}_{q^t(\mathbf{h}^1)}^{CCG} = & \sum_{n=1}^N \sum_{\ell_n=1}^{\mathbf{E}^{(1)}} q^t(\ell_n^{(1)}) \log \theta_{\ell} \\ & + \sum_{n=1}^N \sum_{\ell_n=1}^{\mathbf{E}^{(1)}} \sum_{k_n=1}^{\mathbf{E}^{(1)}} q^t(k_n^{(1)}) \cdot q^t(\ell_n^{(1)}) \log U_{\ell_n^{(1)}}^{\mathbf{W}^{(1)}}(k_n^{(1)}) \end{aligned}$$

where the last term in the equation above can be included in the third term of equation 15 (e.g., add the $l=1$ -addend to first sum).

As last step of the variational recipe, we maximize \mathcal{F} by means of the EM algorithm which iterates E- and M-steps until convergence. The E-step maximizes \mathcal{F} wrt to the posterior distributions given the current status of the model, and in our case reduces to the following updates:

$$\begin{aligned} q^t(k_n^{(L)} = \mathbf{i}) & \propto \left(e^{\sum_{\ell_n} q^t(\ell_n^{(L)}) \log U_{\ell_n^{(L)}}^{\mathbf{W}^{(L)}}(\mathbf{i})} \right) \cdot \pi_{\mathbf{i}}^{(L)}(w_n) \\ q^t(k_n^{(l)} = \mathbf{i}) & \propto \left(e^{\sum_{\ell_n} q^t(\ell_n^{(l)}) \log U_{\ell_n^{(l)}}^{\mathbf{W}^{(l)}}(\mathbf{i})} \right) \cdot \pi_{\mathbf{i}}^{(l)}(\ell_n^{(l-1)}) \\ q^t(\ell_n^{(l)} = \mathbf{i}) & \propto \left(e^{\sum_{k_n} q^t(k_n^{(l)}) \log U_{\mathbf{i}}^{\mathbf{W}^{(l)}}(k_n^{(l)})} \right) \\ & \cdot \left(e^{\sum_{k_n} q^t(k_n^{(l-1)}) \log \pi_{k_n^{(l-1)}}^{(l)}(\mathbf{i})} \right) \quad \forall l = 2 \dots L \end{aligned}$$

The last update can be employed for $l=1$ if the top model is a CCG as well as

$$\theta_{\mathbf{i}}^t \propto \sum_n q(\ell_n^{(l)} = \mathbf{i})$$

In the case we place a CG on the top, the window variable does not depend on the “token” n and we have

$$q^t(\ell^{(1)} = \mathbf{i}) \propto \left(e^{\sum_n \sum_{k_n} q^t(k_n^{(1)}) \log U_{\mathbf{i}}^{\mathbf{W}^{(1)}}(k_n^{(1)})} \right) \cdot \left(e^{\sum_n \sum_{k_n} q^t(k_n^{(1)}) \log \pi_{k_n^{(1)}}^{(1)}(\mathbf{i})} \right)$$

The M step re-estimate the model parameters using these updated posteriors.

$$\pi_{\mathbf{i}}^{(L)}(z) \propto \sum_t \sum_n q^t(k_n^{(L)} = \mathbf{i}) \cdot [w_n^t = z]$$

$$\pi_{\mathbf{i}}^{(l)}(\mathbf{j}) \propto \sum_t \sum_n q^t(k_n^{(l)} = \mathbf{i}) \cdot q^t(\ell_n^{(l+1)} = \mathbf{j})$$

As visible from the last equation, the top level ℓ -variables do not appear, therefore the last update can be employed whatever model we place on top. Variational inference and learning procedure for counting grid-based models utilizes cumulative sums and is slower than training an individual (C-)CG layer by a factor proportional to the number of layers.

Appendix C - Details on user study

In this section, we present the qualitative performance of our models by measuring coherence of micro topics through a *word intrusion* task. The word intrusion task is originally developed to measure the coherence of topics with large scale user study (Chang et al., 2009), and adopted to various models measure the coherence of topics (?).

In the original word intrusion task, six randomly ordered words are presented to a subject. The task of the user is to find the word which is irrelevant with the others. In order to construct a set of words presented to the subject, we first randomly select a target topic from the model. Then we choose the ve most high probability words from that topic. With these five words, an intruder word is randomly selected from low probability words of the target topic but high probability in some other topic. Six words are shuffled and presented to the subject. If the target topic shows a lack of coherence, the subject will be suffering to choose the intruder word.

In order to measure the coherence of micro topics, we slightly modified the standard word intrusion task. First, we randomly sample the location of micro topic, ℓ , from grid. Then we sample three words from the topic of selected location, π_{ℓ} (1×1), from the averaged topic started from the selected location to window of size 2 (2×2), and from the averaged topic started from the selected location to window of size 2 (3×3), respectively.

To prepare data for human subjects, we train four different topic models, LDA, CG, HCG, and HCCG, on randomly

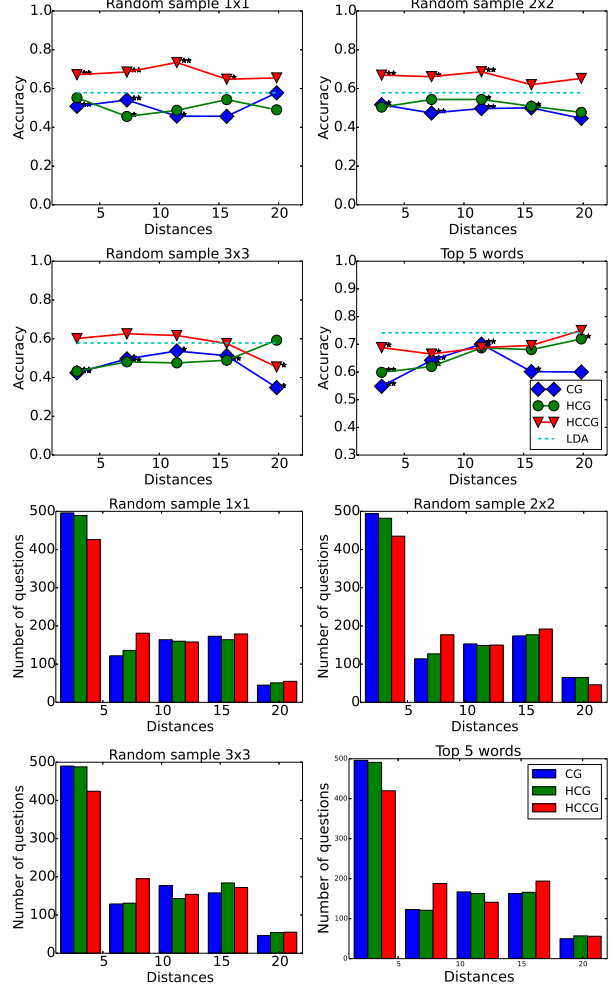


Figure 11. Result of word intrusion task. The significant levels are denoted by * (p -value, * < 0.1 , ** < 0.01)

crawled 10k Wikipedia articles. Amazon Mechanical Turk (<http://www.mturk.com>) is used to perform the word intrusion task.

Table 2. P value between models.

1x1	CG	HCG	HCCG
LDA	8.1E-05	7.7E-03	3.3E-07
CG		2.5E-01	1.1E-16
HCG			1.1E-12
2x2	CG	HCG	HCCG
LDA	1.5E-04	1.6E-03	3.7E-05
CG		5.6E-01	4.2E-13
HCG			2.7E-11
3x3	CG	HCG	HCCG
LDA	2.0E-08	2.0E-08	3.7E-01
CG		1.0E+00	2.9E-09
HCG			2.9E-09
Top K	CG	HCG	HCCG
LDA	2.9E-08	4.5E-05	3.4E-02
CG		6.6E-02	1.7E-05
HCG			1.4E-02

Table 3. Number of questions per each bin.

1x1	1	2	3	4	5
CG	496	122	164	173	45
HCG	489	136	160	164	51
HCCG	426	181	158	179	55
2x2	1	2	3	4	5
CG	494	114	153	174	65
HCG	482	127	149	177	65
HCCG	435	177	150	192	46
3x3	1	2	3	4	5
CG	490	129	177	158	46
HCG	488	131	143	184	54
HCCG	424	195	154	172	55
Top K	1	2	3	4	5
CG	496	123	167	163	50
HCG	491	121	163	166	57
HCCG	420	188	141	194	56